^{4}He(e, $e'p$)^{3}H reaction with full final-state interactions

Sofia Quaglioni,[1,*] Victor D. Efros,[2] Winfried Leidemann,[1] and Giuseppina Orlandini[1]
[1]*Dipartimento di Fisica, Università di Trento, and Istituto Nazionale di Fisica Nucleare, Gruppo Collegato di Trento, I-38050 Povo, Italy*
[2]*Russian Research Centre "Kurchatov Institute," Kurchatov Square, 1, RU-123182 Moscow, Russia*
(Received 2 August 2005; published 21 December 2005)

An *ab initio* calculation of the ^{4}He(e, $e'p$)^{3}H longitudinal response is presented. The full four-body final-state interaction is taken into account by using an integral transform approach with a Lorentzian kernel. The semirealistic nucleon-nucleon potential MTI-III, including the Coulomb force, is the only ingredient of the calculation. The reliability of the direct knock-out hypothesis is discussed in both parallel and nonparallel kinematics. In the former case, lower missing momenta and higher momentum transfers are found to minimize effects beyond the plane-wave impulse approximation. For nonparallel kinematics, the role of antisymmetrization and the final-state interaction become more and more important as the missing momentum increases, raising doubts about the possibility of extracting momentum distributions and spectroscopic factors. The comparison with experimental data is discussed for parallel kinematics, in which a Rosenbluth separation is possible.

DOI: 10.1103/PhysRevC.72.064002 PACS number(s): 21.45.+v, 25.10.+s, 25.30.Fj, 27.10.+h

I. INTRODUCTION

Numerous experimental as well as theoretical investigations of (e, $e'p$) exclusive reactions were extensively performed in the past for both light and heavy nuclei [1–20]. The aim of those studies was to extract information about the structure of the target nucleus, and in particular to access ground-state properties such as spectroscopic factors, shell momentum distributions, etc. However, it is well known that such quantities can only be obtained under the hypothesis that the reaction mechanism is dominated by a direct knock-out of the proton and by neglecting the interaction in the final state. Such assumptions are usually considered more plausible as the momentum transferred by the electron to the system increases and is able to probe "single nucleon" physics. Indeed, in many nuclei the experimental one-body knock-out spectra show very nicely pronounced peaks, hinting of an independent motion of the nucleons in such systems. In these cases, shell momentum distributions and spectroscopic factors were extracted in an attempt to estimate final-state interaction (FSI) effects in various ways. Spectroscopic factors, which are found smaller than 1 (and which are often found considerably far from 1), are interpreted as being due to large "correlation effects" induced by the residual interaction in the ground state of the system.

Unfortunately, up to just recently, the two fundamental assumptions mentioned above could not be checked, because of the impossibility of solving the many-body problem in a quantum mechanically consistent way for both the ground and continuum states. The recent progress made in few-body physics allows us to start investigating these assumptions. For $A = 2$ and 3 the calculations are fully under control [21,22] for both the ground and continuum states, and the problem has been investigated. However, the features of such systems are often considered to be too different from those of a typical many-body nucleus to be taken as testing grounds for validating assumptions on heavier systems.

In the last decade, it has been demonstrated that the procedure to calculate reactions with the help of integral transforms originally proposed in 1985 [23] can be successfully applied in order to overcome the long-standing stumbling block which prevented *ab initio* calculations of high-energy reactions involving four nucleons and more [24–28]. This has been possible thanks to the integral transform with the Lorentz kernel (we will denote it by LIT), proposed in Ref. [29], and recently applied also to the two-body break-up of the four-body system in Ref. [30]. Thus, it is possible now to treat the full dynamics of a reaction to continuum in a nucleus, whose features (binding energy and density) are certainly much closer to those of heavier systems than the deuteron, the triton, or ^{3}He.

It is the purpose of this work to perform a model study of the role of the full treatment of the interaction in the four-body dynamics in the ^{4}He(e, $e'p$)^{3}H reaction and to discuss the plausibility of the direct knock-out and plane-wave assumptions. To this aim, we use the semirealistic potential MTI-III [31] and concentrate on the longitudinal response function, where meson exchange current effects are negligible. This response is accessible experimentally if one performs a Rosenbluth separation in parallel kinematics, and it has been measured in a number of experiments [14,17]. Though the use of a semirealistic potential does not allow one to draw precise conclusions, we believe that a comparison with data may be instructive and we will also comment on that.

In Sec. II, the expression for the (e, $e'p$) cross section is recalled, and the formalism describing the integral transform approach with a Lorentz kernel to exclusive reactions is reviewed. Results are given in Sec. III, while conclusions are summarized in Sec. IV.

*Present address: Department of Physics, P.O. Box 210081, University of Arizona, Tucson, AZ 85721.

II. GENERAL FORMALISM

A. Cross section

The sixfold electrodisintegration cross section of ^{4}He into the two fragments p and ^{3}H is given by [32,33]

$$\frac{d^6\sigma_{p,t}}{dE'd\Omega_{e'}d\mathbf{p}_p} = \sigma_M[V_L S_L(\omega, q, p_p, \theta_p) + V_T S_T(\omega, q, p_p, \theta_p) + V_{LT} S_{LT}(\omega, q, p_p, \theta_p)\cos\phi + V_{TT} S_{TT}(\omega, q, p_p, \theta_p)\cos 2\phi]\,. \quad (1)$$

Here E' and $\Omega_{e'}$ denote the energy and solid angle of the electron after the reaction, σ_M is the Mott cross section, and ϕ denotes the angle between the electron and ejectile planes. Energy and momentum transferred from the electron to the nuclear system are denoted as ω and $\mathbf{q} = q\hat{\mathbf{q}}$. The quantity $\mathbf{p}_p = (p_p, \Omega_p)$ denotes the momentum of the proton detected in coincidence with the electron, and θ_p is the angle between the outgoing proton and $\hat{\mathbf{q}}$. The V_β are kinematical coefficients, and the nuclear dynamics is contained by the structure functions S_β.

Integration over p_p leads to the fivefold cross section

$$\frac{d^5\sigma_{p,t}}{dE'd\Omega_{e'}d\Omega_p} = \int \frac{d^6\sigma_{p,t}}{dE'd\Omega_{e'}d\mathbf{p}_p}\frac{p_p^2}{\left|\frac{\partial E_m}{\partial p_p}\right|}dE_m = \sigma_M \frac{p_p^2}{\left|\frac{\partial E_m}{\partial p_p}\right|}[V_L F_L(\omega, q, \theta_p) + V_T F_T(\omega, q, \theta_p) + V_{LT} F_{LT}(\omega, q, \theta_p)\cos\phi + V_{TT} F_{TT}(\omega, q, \theta_p)\cos 2\phi]\,, \quad (2)$$

where $E_m = \omega - T_p - T_t$ represents the missing energy (T_p and T_t being the proton and triton kinetic energies). The new structure functions F_β are simply given by

$$F_\beta(\omega, q, \theta_p) = \int S_\beta(\omega, q, p_p, \theta_p)dE_m. \quad (3)$$

Notice that since $S_\beta(\omega, q, p_p, \theta_p)$ includes the energy-conserving δ function, the integration over E_m fixes a unique value of p_p for each combination of ω, q, and θ_p.

The total contribution of the (p, t) disintegration channel to the inclusive cross section is

$$\frac{d^3\sigma_{p,t}}{dE'd\Omega_{e'}} = \sigma_M\left[V_L R_L^{p,t}(\omega, q) + V_T R_T^{p,t}(\omega, q)\right], \quad (4)$$

with

$$R_\beta^{p,t}(\omega, q) = \int \frac{2\pi p_p^2}{\left|\frac{\partial E_m}{\partial p_p}\right|} F_\beta(\omega, q, \theta_p)\sin\theta_p d\theta_p\,. \quad (5)$$

In what follows we concentrate on the longitudinal response $F_L(q, \omega, \theta_p)$, representing the response of the system to the electron-nuclear charge interaction. This can be written as

$$F_L(q, \omega, \theta_p) = \sum_{M_t, M_p} |\langle\Psi_{p,t}^-(E_{p,t})|\hat{\rho}(\mathbf{q})|\Psi_\alpha\rangle|^2\,, \quad (6)$$

where the four-body ground state is denoted by Ψ_α, and $\Psi_{p,t}^-$ is the continuum final state of the minus type, pertaining to the proton-triton channel [34] with the relative proton-triton momentum $\mathbf{k} = k\hat{\mathbf{k}}$. The sum goes over the projections M_t and M_p of the fragment total angular momenta in the final state. The continuum states $\Psi_{p,t}^-$ are normalized to $\delta(\mathbf{k} - \mathbf{k}')\delta_{M_t M_t'}\delta_{M_p M_p'}$. The quantity $E_{p,t}$ is the final-state intrinsic energy

$$E_{p,t} = \frac{k^2}{2\mu} + E_t\,, \quad (7)$$

where μ is the reduced mass of the proton-triton system and E_t denotes the ^{3}H ground-state energy.

The initial and final states are connected by the nuclear charge operator $\hat{\rho}$, which we take in its nonrelativistic form

$$\hat{\rho}(\mathbf{q}) = \sum_{j=1}^{4} G_E^p \frac{1 + \tau_j^3}{2}\exp(i\,\mathbf{q}\cdot\mathbf{r}_j)\,. \quad (8)$$

Here τ_j^3 denotes the third component of the j-th nucleon isospin, $\mathbf{r}_j$ represents the position of the j-th nucleon with respect to the center of mass of the four-body system, and G_E^p is the proton electric form factor. In comparing our results with experimental data, we will use the proton form factor $\tilde{G}_E^p = G_E^p/(1 + (q^2 - \omega^2)/4m_p^2)^{1/2}$ (containing first-order relativistic correction) with G_E^p in the usual dipole parametrization.

The main difficulty in the calculation of F_L is represented by the continuum wave function $\Psi_{p,t}^-(E_{p,t})$ in the transition matrix element

$$T_{p,t}(E_{p,t}) = \langle\Psi_{p,t}^-(E_{p,t})|\hat{\rho}|\Psi_\alpha\rangle. \quad (9)$$

With the integral transform method [23] using the Lorentz kernel [29,35], one is able to perform an *ab initio* calculation of this transition matrix element in a large energy range without dealing with the continuum solutions of the four-body Schrödinger equation. How this is possible has been described in Ref. [23] and will be briefly summarized in the next subsection. Further details can be found in [30,35–37].

B. The LIT method for exclusive reactions

The LIT approach to exclusive reactions consists of calculating the transition matrix element of the perturbation $\widehat{O}$ between the initial (Ψ_0) and final (Ψ_f^-) states

$$T_f(E_f) = \langle\Psi_f^-(E_f)|\widehat{O}|\Psi_0\rangle, \quad (10)$$

without calculating $\Psi_f^-(E_f)$.

In general, denoting with a and b the two fragments containing n_a and $n_b = A - n_a$ nucleons, respectively, and with H the full nuclear Hamiltonian, we have the following formal expression for $\Psi_{f=a,b}^-(E_{f=a,b})$ in terms of the "channel state" $\phi_{f=a,b}^-(E_{f=a,b})$ [34]

$$|\Psi_{a,b}^-(E_{a,b})\rangle = \widehat{\mathcal{A}}|\phi_{a,b}^-(E_{a,b})\rangle + \frac{1}{E_{a,b} - i\varepsilon - H}\widehat{\mathcal{A}}\mathcal{V}|\phi_{a,b}^-(E_{a,b})\rangle, \quad (11)$$

where $\widehat{\mathcal{A}}$ is an antisymmetrization operator. In the case that at least one of the fragments is chargeless, the channel wave function $\phi_{a,b}^-(E_{a,b})$ is the product of the internal wave functions of the fragments and of their relative free motion. Correspondingly, $\mathcal{V}$ in Eq. (11) is the sum of all interactions

between particles belonging to different fragments. If both fragments are charged, as in our case, $\phi^-_{a,b}(E_{a,b})$ is chosen to account for the average Coulomb interaction between them, and the plane wave describing their relative motion is replaced by the Coulomb function of the minus type. Correspondingly, $\mathcal{V}$ in Eq. (11) is the sum of all interactions between particles belonging to different fragments after subtraction of the average Coulomb interaction, already considered via the Coulomb function. We write $\phi^-_{a,b}(E_{a,b})$ in the partial wave expansion form

$$\phi^-_{a,b}(E_{a,b}) = \frac{\Phi_a(1,\ldots,n_a)\Phi_b(n_a+1,\ldots,A)}{(2\pi)^{3/2}} \times 4\pi \sum_{\ell=0}^{\infty}\sum_{m=-\ell}^{\ell} i^\ell e^{-i\delta_\ell(k)} \frac{w_\ell(k;r)}{kr} Y_{\ell m}(\Omega_r) Y^*_{\ell m}(\Omega_k). \tag{12}$$

Here $\Phi_a(1,\ldots,n_a)$ and $\Phi_b(n_a+1,\ldots,A)$ are the internal wave functions of the fragments, $\mathbf{r} = (r, \Omega_r) = \mathbf{R}^a_{\rm cm} - \mathbf{R}^b_{\rm cm}$ represents the distance between them, and the energy of the relative motion is $k^2/2\mu = E_{a,b} - E_a - E_b$, where E_a and E_b are the fragment ground-state energies. The functions $w_\ell(k;r)$ are the regular Coulomb wave functions of order ℓ, and $\delta_\ell(k)$ are the Coulomb phase shifts [34]. The internal wave functions of the fragments are assumed to be antisymmetric and normalized to unity, so that the properly normalized continuum wave function in Eq. (11) is obtained via application of the antisymmetrization operator. For $n_a = 1$, this has the form

$$\widehat{\mathcal{A}} = \frac{1}{\sqrt{A}}\left[1 - \sum_{j=2}^{A} \mathcal{P}_{1j}\right], \tag{13}$$

where $\mathcal{P}_{ij}$ are particle permutation operators [34].

When one inserts Eq. (11) into Eq. (10), the transition matrix element becomes the sum of two pieces: A Born term,

$$T^{\rm Born}_{a,b}(E_{a,b}) = \langle \phi^-_{a,b}(E_{a,b}) | \widehat{\mathcal{A}}\widehat{O} | \Psi_0 \rangle, \tag{14}$$

and an FSI-dependent term,

$$T^{\rm FSI}_{a,b}(E_{a,b}) = \langle \phi^-_{a,b}(E_{a,b}) | \mathcal{V}\widehat{\mathcal{A}} \frac{1}{E_{a,b} + i\varepsilon - H} \widehat{O} | \Psi_0 \rangle. \tag{15}$$

While the Born term is rather simple to deal with, the determination of the FSI-dependent matrix element is rather complicated. Within the LIT approach, this term is treated as outlined in the following.

In Eq. (15) one inserts the completeness relation of the Hamiltonian eigenstates $\Psi_\nu(E_\nu)$ [labeled by channel quantum numbers ν and normalized as $\langle \Psi_\nu | \Psi_{\nu'} \rangle = \delta(\nu - \nu')$]

$$T^{\rm FSI}_{a,b}(E_{a,b}) = \sum\!\!\!\!\!\!\int d\nu \, \langle \phi^-_{a,b}(E_{a,b}) | \mathcal{V}\widehat{\mathcal{A}} | \Psi_\nu(E_\nu) \rangle \times \frac{1}{E_{a,b} + i\varepsilon - E_\nu} \langle \Psi_\nu(E_\nu) | \widehat{O} | \Psi_0 \rangle. \tag{16}$$

Defining $F_{a,b}(E)$ as

$$F_{a,b}(E) = \sum\!\!\!\!\!\!\int d\nu \langle \phi^-_{a,b}(E_{a,b}) | \mathcal{V}\widehat{\mathcal{A}} | \Psi_\nu(E_\nu) \rangle \times \langle \Psi_\nu(E_\nu) | \widehat{O} | \Psi_0 \rangle \delta(E - E_\nu), \tag{17}$$

one has

$$T^{\rm FSI}_{a,b}(E_{a,b}) = \int_{E^-_{\rm th}}^{\infty} \frac{F_{a,b}(E)}{E_{a,b} + i\varepsilon - E} dE = -i\pi F_{a,b}(E_{a,b}) + \mathcal{P}\int_{E^-_{\rm th}}^{\infty} \frac{F_{a,b}(E)}{E_{a,b} - E} dE, \tag{18}$$

where $E_{\rm th}$ is the lowest excitation energy in the system, i.e., the break-up threshold energy.

The function $F_{a,b}$ contains information on all the eigenstates Ψ_ν for the whole eigenvalue spectrum of H. It is obtained by its Lorentz integral transform

$$L[F_{a,b}](\sigma) = \int_{E^-_{\rm th}}^{\infty} \frac{F_{a,b}(E)}{(E-\sigma_R)^2 + \sigma_I^2} dE = \langle \widetilde{\Psi}_2(\sigma) | \widetilde{\Psi}_1(\sigma) \rangle, \tag{19}$$

where

$$\widetilde{\Psi}_1(\sigma) = (H-\sigma)^{-1}\widehat{O}|\Psi_0\rangle, \quad \widetilde{\Psi}_2(\sigma) = (H-\sigma)^{-1}\widehat{\mathcal{A}}\mathcal{V}|\phi^-_{a,b}(E_{a,b})\rangle, \tag{20}$$

and $\sigma = \sigma_R + i\sigma_I$. Equation (19) shows that $L\left[F_{a,b}\right](\sigma)$ can be calculated without explicit knowledge of $F_{a,b}$, provided that one solves the two equations

$$(H-\sigma)|\widetilde{\Psi}_1\rangle = \widehat{O}|\Psi_0\rangle, \tag{21}$$

$$(H-\sigma)|\widetilde{\Psi}_2\rangle = \widehat{\mathcal{A}}\mathcal{V}|\phi^-_{a,b}(E_{a,b})\rangle, \tag{22}$$

which differ in the source terms only. It is easy to show that $\widetilde{\Psi}_1$ and $\widetilde{\Psi}_2$ have finite norms. When solving Eqs. (21) and (22), it is sufficient to require that the solutions are localized, and no other boundary conditions are to be imposed. Therefore, "bound state" techniques can be applied.

We use an expansion over a basis set of localized functions consisting of correlated hyperspherical harmonics (CHH) multiplied by hyperradial functions. As discussed in [26] for the case of the total ^{4}He photoabsorption cross section, special attention has to be paid to the convergence of such expansions. A rather large number of basis states is necessary in order to reach convergence, thus leading to large Hamiltonian matrices. Instead of using a time-consuming inversion method, we directly evaluate the scalar products in (19) with the Lanczos technique, as explained in Ref. [38].

After having calculated $L[F_{a,b}](\sigma)$, one obtains the function $F_{a,b}(E)$ and, thus, $T_{a,b}(E_{a,b})$ via the inversion of the LIT, as described in [39].

In the next section, results obtained by means of Eq. (14) will be denoted by PWIAS. The label PWIA (plane-wave impulse approximation) will indicate that in Eq. (14) the antisymmetrization operator $\widehat{\mathcal{A}}$ has been neglected. We remind the reader that in this case, the structure function $F_L^{p,t}$ turns out to be factorized in terms of the proton form factor and a function $n(|\mathbf{q} - \mathbf{p}_\mathbf{p}|)$, which is the Fourier transform of the overlap between the ^{4}He and ^{3}H ground-state wave functions.

III. RESULTS

As already mentioned, the ground states of ^{4}He and ^{3}He as well as the $\widetilde{\Psi}$ in Eqs. (21) and (22) are calculated using the

CHH expansion method. In order to speed up the convergence, state-independent correlations are introduced, as in [24]. We use the MTI-III [31] potential and identical CHH expansions for the ground-state wave functions of ^{4}He and of the three-nucleon systems, as in [26] and [40], respectively.

We calculate the transition matrix elements (14) and (15) in the form of partial-wave expansions. When one substitutes the expansion (12) and the expansion

$$\hat{\rho}(\mathbf{q}) = \sum_{LM} Y^*_{LM}(\Omega_q)\hat{\rho}_{LM}(q) \tag{23}$$

of the charge operator (8) into the Born amplitude (14) and into the right-hand sides of Eqs. (21) and (22), one finds that in our case of central nucleon-nucleon (*NN*) forces the transition matrix element (9) turns into a sum over L [L is equal to the l in (12)] of partial transition matrix elements multiplied by the factors

$$\sum_{M=-L}^{L} Y_{LM}(\Omega_k)Y^*_{LM}(\Omega_q) = (4\pi)^{-1}(2L+1)P_L(\hat{\mathbf{k}}\cdot\hat{\mathbf{q}}). \tag{24}$$

These factors determine the dependence of the cross section on θ_p. The dynamic equations are split with respect to orbital momentum L, and they are M independent. The multipole transitions of the charge operator in Eq. (8) are taken into account up to a maximal value of $L_{\rm Born} = 20$ and $L_{\rm FSI} = 6$ for the Born and FSI terms, respectively. (The relatively low value of $L_{\rm FSI}$ is due to the fact that the FSI does not affect the final-state higher partial waves significantly.) Correspondingly, Eqs. (21) and (22) are solved for the different values of L, running from 0 to $L_{\rm FSI}$. Since the excitation operator induces both isoscalar and isovector transitions, the hyperspherical harmonics (HH) entering the calculation are characterized by the quantum numbers L, S, T such that $S = 0$ and $T = 0, 1$. In the calculation involving L up to 4, the maximal value of the grand-angular quantum number $K_{\rm max}$ is taken to be 7 (odd multipoles) or 8 (even multipoles), the only exception being the $L = 1$ multipole in the $T = 0$ channel, for which $K_{\rm max} = 9$ has been used. For $L = 5$ and $L = 6$ $K_{\rm max}$ is equal to 9 and 10, respectively. These values of the grand-angular quantum number provide the convergence of the various LIT's of Eq. (19) with an uncertainty in the response function (6) of less than 1%. In addition, for $K_{\rm max} = 9$ and 10, a selection of states has been performed with respect to the permutational symmetry types of the HH. Among the HH entering the expansion, those belonging to the irreducible representations $[f] = [2]$ and $[f] = [-]$ [24,41] of the four-particle permutation group $\mathbf{S}_4$ can be neglected in the calculation of the LIT for K values higher than 7 (odd multipoles) and 8 (even multipoles).

We start by illustrating the contributions of the proton-triton channel and of the mirror channel due to the neutron-^{3}He break-up to the total inclusive response function. This comparison serves as a test of the correctness of the results. In fact, below the threshold for the disintegration of ^{4}He into proton, neutron, and deuteron for the isovector case and into two deuterons for the isocalar case, the two results should coincide. The neutron-^{3}He response $R^{n,h}_L(\omega, q)$ has been calculated along the same lines as described above, except that in the channel state $\phi^-_{f=a,b}(E_{f=a,b})$ of Eq. (11) the relative motion is given by a plane wave. We choose to compare the sum of $R^{p,t}_L(\omega, q)$ and $R^{n,h}_L(\omega, q)$ for the multipoles $L = 0, T = 1$ and $L = 2, T = 0$ (two of the multipoles which contribute most) with the total inclusive response calculated for the same multipoles. This comparison is shown in Fig. 1. Considering that the calculation of the total longitudinal response proceeds in a very different way, i.e., only by inversion of the norm of $\tilde{\Psi}_1$ [24], this comparison confirms the correctness of the calculation. Besides the degree of accuracy of the results, one also notices that for these multipoles the proton-triton and neutron-^{3}He channels dominate much beyond those thresholds.

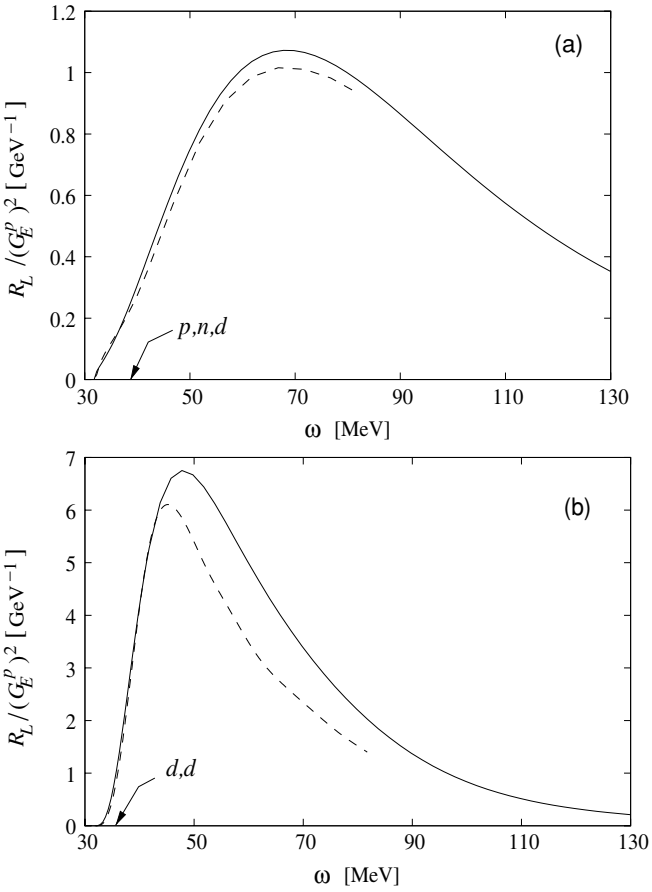

FIG. 1. $T = 1, L = 0$ [panel (a)] and $T = 0, L = 2$ [panel (b)] components of the inclusive response (solid line) compared to those of $R^{p,t}_L + R^{n,h}_L$ [see Eq. (5)] (dashed line) for $q = 300$ MeV/c. Arrows indicate the proton-neutron-deuteron (p, n, d) and deuteron-deuteron (d, d) break-up thresholds.

A. Parallel kinematics

Our study of $F_L(\omega, q, \theta_p)$ focuses first on the parallel kinematics of Ref. [17], where a Rosenbluth separation has been performed. In the columns 2–4 of Table I, we list the values of q, ω and the modulus of missing momentum $\mathbf{p}_m = \mathbf{q} - \mathbf{p}_p$ of the kinematics we have chosen to analyze (labeled by Kin. No. in column 1). The values of the experimental energies and momentum transfers are illustrated in Fig. 2 as

TABLE I. ^{4}He$(e, e'p)^3$H longitudinal response function of Eq. (6) in PWIA for the parallel kinematics of Fig. 2. The relative PWIAS and FULL effects, $\Delta_X = (X - \text{PWIA})/\text{PWIA}$, are also listed.

Kin. No.	q (MeV/c)	ω (MeV)	PWIA p_m (MeV/c)	PWIA $F_L/\left(G_E^p\right)^2$ [(GeV/c)$^{-3}$sr^{-1}]	Δ_{PWIAS} (%)	Δ_{FULL} (%)
1	299	57.78	+30	185.2	+9.3	−39.6
2	380	83.13	+30	185.2	+1.2	−20.1
3	421	98.19	+30	185.2	+0.0	−12.8
4	299	98.70	−90	100.0	+4.5	−43.4
5	380	65.06	+90	100.0	+3.9	−16.6
6	544	126.6	+90	100.0	−1.1	+11.4
7	572	137.82	+90	100.0	−1.9	+11.5
8	650	175.67	+90	100.0	−1.7	+10.8
9	680	146.48	+190	14.63	−4.4	+52.1

points in the q-ω plane and labeled with the corresponding numbers. In the same figure, their positions with respect to the ridge $\omega = q^2/(2m_p)$ are shown (m_p is the proton mass). The value of the final-state intrinsic energy $E_{p,t}$, which is the input of the calculation, has been obtained by calculating first the relative momentum $\mathbf{k}$ from the relation

$$\mathbf{k} = \mu\left(\frac{\mathbf{p}_p}{m_p} - \frac{(\mathbf{q} - \mathbf{p}_p)}{m_t}\right) \tag{25}$$

and then using Eq. (7).

In column 5 of Table I, the PWIA results are listed. In this approximation and in an independent particle model of ^{4}He, the PWIA result represents the probability that the proton in the s shell of ^{4}He has momentum p_m. Therefore, one has constant values for Kin. Nos. 1–3 and 4–8. The integral over all values of $\mathbf{p}_m$ gives the "spectroscopic factor" for that shell, which for this potential turns out to be 0.88 [42] (this value can be compared with 0.84 obtained using a realistic potential like AV18 and Urbana IX [43–45]).

In Table I, the effects of antisymmetrization and FSI are also shown as percentages of the PWIA values (the results denoted as FULL include both effects). In general, one notices small effects of antisymmetrization for almost all cases as one would expect for kinematics with p_m much smaller than q. Nevertheless, for the kinematics at lower energies, these effects can increase up to about 10%. The role of FSI is much more important at low q. One notices that (i) for the kinematics close to the $\omega = q^2/(2m_p)$ ridge, FSI effects decrease for increasing q; (ii) Kin. Nos. 4 and 9, which are more distant from the ridge $\omega = q^2/(2m_p)$, present a rather high contribution of FSI; and (iii) at higher momenta and in the lower energy side of the ridge, FSI enhances the PWIA results. This latter effect goes in the opposite direction compared to previous estimates based either on optical potentials and an orthogonalization procedure [46], or on diagrammatic expansions [47].

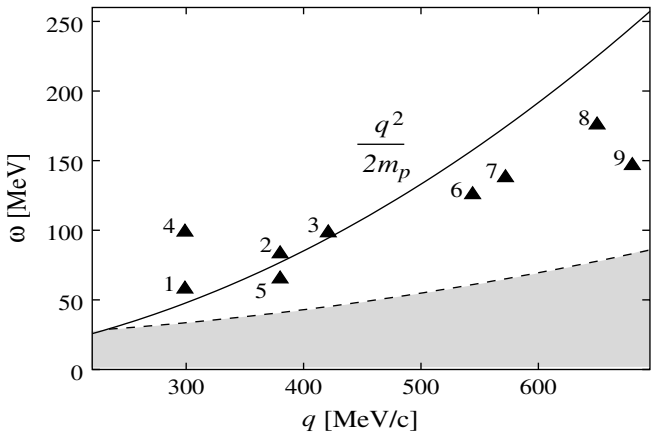

FIG. 2. Position of the various kinematics of Table I with respect to the $\omega = q^2/(2m_p)$ ridge. Shaded area represents the region below the break-up threshold, where the cross section is zero.

Observation (iii) is consistent with previous *ab initio* calculations of the inclusive longitudinal response function in ^{2}H [21], ^{3}He [48], and ^{4}He [24]. In these cases, one finds that the longitudinal responses at constant q values, calculated with and without FSI, cross at an ω value of approximately $q^2/(2m_p)$. The fact that the crossing happens just along that ridge is probably due to the different effects of the potential in the initial and final states with respect to the free one-body knock-out model, as explained in the following. In the one-body knock-out model, the PWIA peak energy is $\omega_{\text{peak}} = q^2/(2m_p) + \Delta$. The positive quantity Δ is the difference between the binding energies of ^{4}He and ^{3}H and can be considered as a "ground-state effect" of the potential. One can argue that the additional effect of the potential in the final state would lead to $\omega_{\text{peak}} = q^2/(2m_p) + \Delta - \bar{V}$, where $\bar{V}$ represents the mean interaction energy between the proton and triton in the final state interaction zone ($\bar{V}$ will be attractive). Therefore, the PWIA and FSI curves should intersect at an energy smaller than $q^2/(2m_p) + \Delta$. To a good accuracy, this value turns out to be just $q^2/(2m_p)$. Of course such a comparison between inclusive and exclusive results is justified only in case of sufficiently low p_m as is the case for the kinematics listed in Table I.

Similar PWIAS and FSI effects are also found for Kin. Nos. 6 and 9 in the two-body break-up results of ^{3}He [49].

It is a common belief that the kinematical regions at lower-energy and higher-momentum transfers are the privileged ones for investigating the ground-state short-range correlation effects. Our results show that if one relies on approximate approaches to estimate the FSI effects one might underestimate considerably the momentum distributions at high p_m extracted from experiments in those kinematical regions.

As stated above, the aim of the present work is mainly to study the relative effects of antisymmetrization and FSI, which are often treated approximately, via a complete solution of the quantum mechanical few-body problem. We have conducted this study using a semirealistic potential model. Nevertheless, it is interesting to compare our results with experimental data. This comparison is shown in Table II. Except for the case at the lowest ω and q (Kin. No. 1), where there is a good agreement, our results are almost systematically higher than data. The difference ranges from about 30% for the kinematics closer to the quasielastic ridge to about 70% and even 100% for the other. This comparison is better illustrated in Fig. 3.

TABLE II. ^{4}He$(e, e'p)^3$H longitudinal response function. Theoretical results (FULL) compared with the experimental values of Ref. [17]: Statistical and systematic uncertainties are indicated (±stat. ±syst.).

Kin. No.	F_L [(GeV/c)$^{-3}$ sr^{-1}]			
	Expt.			FULL
1	59.0	±2.0	±2.2	66.4
2	49.6	±2.1	±2.1	66.9
3	46.2	±2.5	±2.2	62.7
4	27.8	±1.0	±1.2	34.9
5	28.4	±1.2	±1.3	37.2
6	14.8	±1.4	±1.2	25.9
7	16.0	±1.5	±1.3	23.0
8	9.96	±1.29	±1.15	16.3
9	1.35	±0.22	±0.22	2.73

One can see that while FSI tends to bring theoretical results closer to data for the kinematics at lower momenta (Kin. Nos. 1–5), it affects in the opposite direction those at higher q (Kin. Nos. 6–9), with the largest effect for Kin. No. 9, which corresponds to the highest q and p_m values. This is a delicate region, where cross sections are small, and potential dependence and relativistic effects neglected here might play a major role.

B. Nonparallel kinematics

It is interesting to investigate the above effects also in nonparallel kinematics. At fixed energy and momentum transfer, one can access different p_m varying θ_p. Therefore, in PWIA the response reflects a proton momentum distribution. In the following we will show how antisymmetrization and FSI can spoil this interpretation. For the (ω, q) values of Table I, results for nonparallel kinematics are shown in Fig. 4 as functions of p_m. In the upper panel one can clearly see that the mere antisymmetrization effect does not allow the interpretation of the response in terms of momentum distribution beyond certain values of p_m, depending on the kinematics. These values are rather small (around 1 fm^{-1}) for the kinematics at lower-momentum transfer and can reach 2 fm^{-1} for those at higher q. This is, of course, discouraging for a study of the short-range correlations, which contribute mainly to the higher tail of the momentum distribution.

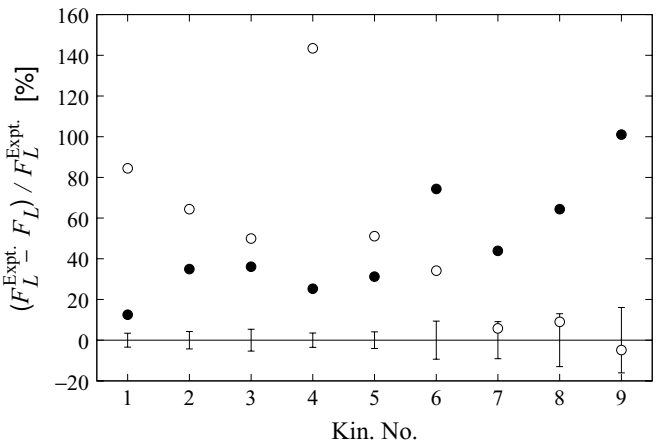

FIG. 3. Percentage deviation from the experimental values of Ref. [17]: PWIA (open circles), FULL (solid circles).

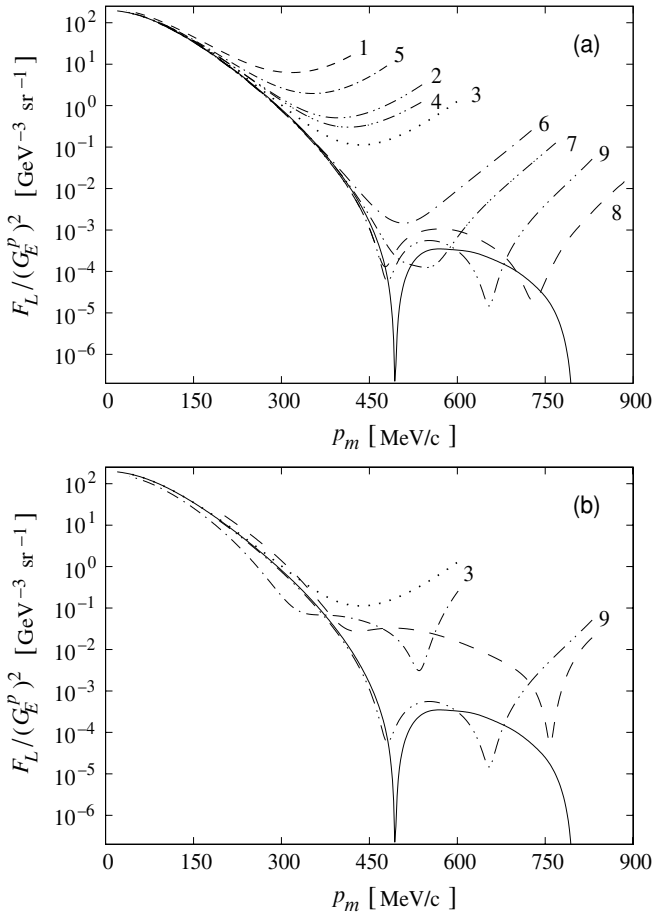

FIG. 4. ^{4}He$(e, e'p)^3$H longitudinal response function of Eq. (6) as function of p_m. (a) PWIAS for the different (ω, q) values of Table I labeled with the corresponding numbers; (b) PWIAS (dotted and dot-dot-dashed line) and FULL (dashed and dot-dashed line) results for the (ω, q) values of Kin. Nos. 3 and 9 of Table I. The solid line represents the PWIA.

Figure 4 shows that antisymmetrization effects tend to fill the minimum of the response in PWIA. We illustrate the FSI effect in the lower panel, where we have chosen Kin. No. 3 with a smaller and Kin. No. 9 with a larger q value. As in parallel kinematics, FSI tends to decrease the response in the former case and to enhance it in the latter. It is interesting to see that some minima reappear and some are filled when FSI is included.

For a better understanding of the situation, it is instructive to plot the matrix elements calculated from Eqs. (10), (14), and (15). As an example, we choose Kin. No. 3. In Fig. 5(a) our results for $T_{p,t}^{\rm Born}$ are shown for PWIA and PWIAS. Moreover, in order to see the difference between an independent particle model and a correlated one, we also show the corresponding results obtained in an harmonic oscillator (h.o.) model. (The

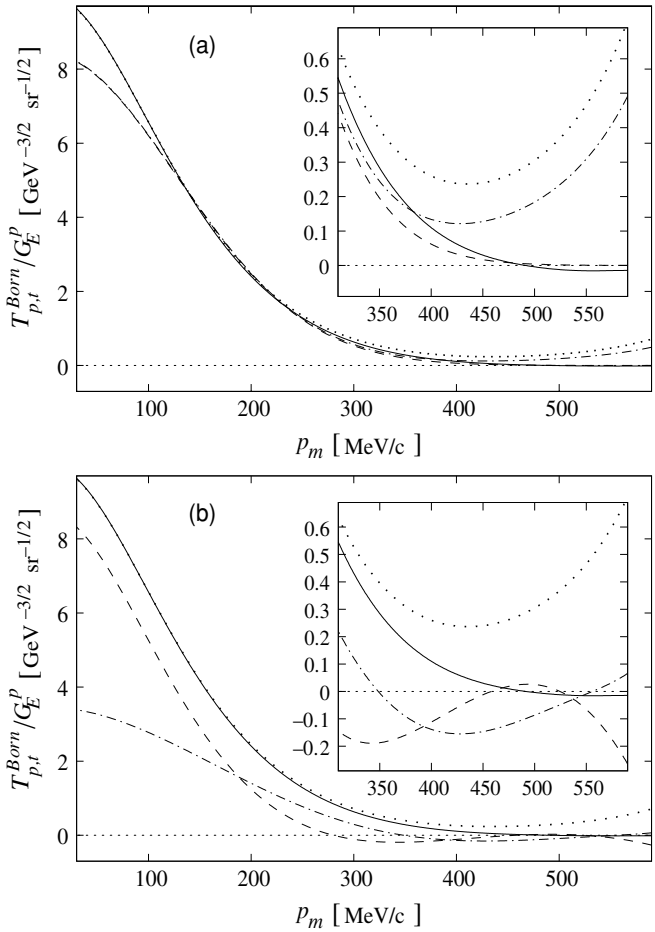

FIG. 5. Matrix element $T_{p,t}(E)$ of Eq. (9) in nonparallel kinematics, for q and ω of Kin. No. 3, as function of p_m. (a) h.o. model: PWIA (dashed line), PWIAS (dotted line); MTI-III potential model: PWIA (full line), MTI-III, PWIAS (dot-dashed line). (b): MTI-III potential model: Real (dashed line) and imaginary (dot-dashed line) parts of the FULL matrix element. PWIA and PWIAS results as in (a).

h.o. parameters have been fixed to the radii of ^{4}He and ^{3}H). Since the MTI-III potential has a rather strongly repulsive core, the comparison exhibits the effect of ground-state short-range correlations. One readily sees that at low p_m the MTI-III potential gives a 15% quenching. The tail region is amplified in the inset. The results of the two models have similar behaviors with increasing p_m, both in PWIA and PWIAS [see also inset of Fig. 5(a)]. However, while the h.o. PWIA matrix element remains always positive, the corresponding one for MTI-III crosses the zero axis, giving rise to the minimum visible in Fig. 4. The minimum is then washed out by the antisymmetrization effect.

In Fig. 5(b) the additional role of FSI is shown. In this case, the total matrix element $T^{\rm Born}_{p,t} + T^{\rm FSI}_{p,t}$ is complex. Real and imaginary parts are shown and compared to the Born result with the MTI-III potential. In the inset, the complicated interplay of the different contributions is illustrated. It is evident that FSI leads to a result close to zero for a rather wide p_m range, causing appearances and disappearances of minima in the cross section. A more realistic interaction may change the present picture in that kinematical region considerably. Nonetheless, this model study points out that it might be difficult to search for ground-state correlation effects at high p_m values within a PWIA picture.

IV. CONCLUSIONS

We have presented the results of an *ab initio* calculation of the ^{4}He$(e, e'p)^3$H longitudinal response obtained by means of the integral transform method with a Lorentz kernel. For the *NN* interaction, we have used the MTI-III potential model. The aim has been to investigate the limits of the PWIA approximation (factorization in terms of momentum distribution) due to the effects of antisymmentrization and FSI. We have analyzed the situation for the parallel kinematics investigated in the experiments of Ref. [17] and for two nonparallel kinematics. Our model study has shown that the factorized approach (PWIA) might be a reasonable approximation for small missing momenta (below 0.5 fm^{-1}) and higher-momentum transfers (above 2 fm^{-1}). Unfortunately, the situation for higher missing momenta becomes much more involved. Both antisymmetrization effects and FSI play an important role. In particular, for non-parallel kinematics their entanglement can give rise to drastic deviations from the PWIA result. Furthermore, one may expect considerable sensitivity to nuclear dynamics here. On the one hand, this result can be considered discouraging in relation to the possibility to "measure" directly short-range ground-state correlations. On the other hand, it is possible that because of the sensitivity of the response to all effects, those kinematical regions are ideal to study potential model dependence, including perhaps that due to three-body forces. However, FSI has to be treated in a proper way, and realistic interactions have to be used before definite conclusions can be drawn. The integral transform approach with a Lorentz kernel is a promising approach to pursuing such studies.

ACKNOWLEDGMENTS

We thank B. R. Barrett for critical reading of the manuscript. This work was supported by the grant COFIN03 of the Italian Ministry of University and Research. V.D.E. acknowledges support from the RFBR, Grant 05-02-17541. S. Q. acknowledges partial support by the NSF grant PHY0244389. A large part of the numerical calculations were performed at the computer center CINECA (Bologna).

[1] S. Frullani and J. Mougey, Adv. Nucl. Phys. **14**, 1 (1984).
[2] R. W. Lourie, H. Baghaei, W. Bertozzi, K. I. Blomqvist, J. M. Finn, C. E. Hyde-Wright, N. Kalantar-Nayestanaki, J. Nelson, S. Kowalski, C. P. Sargent *et al.*, Phys. Rev. Lett. **56**, 2364 (1986).
[3] G. van der Steenhoven, H. P. Blok, J. F. J. van den Brand, T. de Forest Jr., J. W. A. den Herder, E. Jans, P. H. M. Keizer, L. Lapikás, P. J. Mulders, E. N. M. Quint *et al.*, Phys. Rev. Lett. **57**, 182 (1986).

[4] G. van der Steenhoven, A. M. van den Berg, H. P. Blok, S. Boffi, J. F. J. van den Brand, R. Ent, T. de Forest Jr., C. Giusti, J. W. A. den Herder, E. Jans *et al*., Phys. Rev. Lett. **58**, 1727 (1987).
[5] P. E. Ulmer, H. Baghaei, W. Bertozzi, K. I. Blomqvist, J. M. Finn, C. E. Hyde-Wright, N. Kalantar-Nayestanaki, S. Kowalski, R. W. Lourie, J. Nelson *et al*., Phys. Rev. Lett. **59**, 2259 (1987).
[6] E. Jans, M. Bernheim, M. K. Brussel, G. P. Capitani, E. De Sanctis, S. Frullani, F. Garibaldi, J. Morgenstern, J. Mougey, I. Sick *et al*., Nucl. Phys. **A475**, 687 (1987).
[7] D. Reffay-Pikeroen, M. Bernheim, S. Boffi, G. P. Capitani, E. De Sanctis, S. Frullani, F. Garibaldi, A. Gérard, C. Giusti, H. Jackson *et al*., Phys. Rev. Lett. **60**, 776 (1988).
[8] C. Marchand, M. Bernheim, P. C. Dunn, A. Gérard, J. M. Laget, A. Magnon, J. Morgenstern, J. Mougey, J. Picard, D. Reffay-Pikeroen, S. Turck-Chieze *et al*., Phys. Rev. Lett. **60**, 1703 (1988).
[9] J. F. J. van den Brand, H. P. Blok, R. Ent, E. Jans, G. J. Kramer, J. B. J. M. Lanen, L. Lapikás, E. N. M. Quint, G. van der Steenhoven, and P. K. A. de Witt Huberts, Phys. Rev. Lett. **60**, 2006 (1988).
[10] G. van der Steenhoven, H. P. Blok, E. Jans, M. de Jong, L. Lapikás, E. N. M. Quint, and P. K. A. de Witt Huberts, Nucl. Phys. **A480**, 547 (1988).
[11] G. V. D. Steenhoven, H. P. Blok, E. Jans, L. Lapikás, E. N. M. Quint, and P. K. A. de Witt Huberts, Nucl. Phys. **A484**, 445 (1988).
[12] J. W. A. den Herder, H. P. Blok, E. Jans, P. H. M. Keizer, L. Lapikás, E. N. M. Quint, G. V. D. Steenhoven, and P. K. A. de Witt Huberts, Nucl. Phys. **A490**, 507 (1988).
[13] J. B. J. M. Lanen, A. M. van den Berg, H. P. Blok, J. F. J. van den Brand, C. T. Christou, R. Ent, A. G. M. van Hees, E. Jans, G. J. Kramer, L. Lapikás, D. R. Lehman *et al*., Phys. Rev. Lett. **62**, 2925 (1989).
[14] A. Magnon, M. Bernheim, M. K. Brussel, G. P. Capitani, E. De Sanctis, S. Frullani, F. Garibaldi, A. Gerard, H. E. Jackson, J. M. Legoff *et al*., Phys. Lett. **B222**, 352 (1989).
[15] J. B. J. M. Lanen, H. P. Blok, E. Jans, L. Lapikás, G. van der Steenhoven, and P. K. A. de Witt Huberts, Phys. Rev. Lett. **64**, 2250 (1990).
[16] J. F. J. van den Brand, H. P. Blok, H. J. Bulten, R. Ent, E. Jans, G. J. Kramer, J. M. Laget, J. B. J. M. Lanen, L. Lapikás, J. S. Roebers *et al*., Phys. Rev. Lett. **66**, 409 (1991).
[17] J. E. Ducret, M. Bernheim, M. K. Brussel, G. P. Capitani, J. F. Danel, E. De Sanctis, S. Frullani, F. Garibaldi, F. Ghio, H. E. Jackson *et al*., Nucl. Phys. **A556**, 373 (1993).
[18] M. Leuschner, J. R. Calarco, F. W. Hersman, E. Jans, G. J. Kramer, L. Lapikás, G. van der Steenhoven, P. K. A. de Witt Huberts, H. P. Blok *et al*., Phys. Rev. C **49**, 955 (1994).
[19] J. M. Le Goff, M. Bernheim, M. K. Brussel, G. P. Capitani, J. F. Danel, E. De Sanctis, S. Frullani, F. Garibaldi, A. Gerard, M. Jodice *et al*., Phys. Rev. C **50**, 2278 (1994).
[20] J. J. van Leeuwe, H. P. Blok, J. F. J. van den Brand, H. J. Bulten, G. E. Dodge, R. Ent, W. H. A. Hesselink, E. Jans, W. J. Kasdorp, J. M. Laget *et al*., Phys. Rev. Lett. **80**, 2543 (1998).
[21] H. Arenhövel, W. Leidemann, and E. L. Tomusiak, Eur. Phys. J. A **23**, 147 (2005).
[22] J. Golak, H. Witala, R. Skibihski, W. Glöckle, A. Nogga, and H. Kamada, Phys. Rev. C **70**, 034005 (2004).
[23] V. D. Efros, Yad. Fiz. **41**, 1498 (1985) [Sov. J. Nucl. Phys. **41**, 949 (1985)].
[24] V. D. Efros, W. Leidemann, and G. Orlandini, Phys. Rev. Lett. **78**, 432 (1997).
[25] V. D. Efros, W. Leidemann, and G. Orlandini, Phys. Rev. Lett. **78**, 4015 (1997).
[26] N. Barnea, V. D. Efros, W. Leidemann, and G. Orlandini, Phys. Rev. C **63**, 057002 (2001).
[27] S. Bacca, M. A. Marchisio, N. Barnea, W. Leidemann, and G. Orlandini, Phys. Rev. Lett. **89**, 052502 (2002).
[28] S. Bacca, H. Arenhövel, N. Barnea, W. Leidemann, and G. Orlandini, Phys. Lett. **B603**, 159 (2004).
[29] V. D. Efros, W. Leidemann, and G. Orlandini, Phys. Lett. **B338**, 130 (1994).
[30] S. Quaglioni, W. Leidemann, G. Orlandini, N. Barnea, and V. D. Efros, Phys. Rev. C **69**, 044002 (2004).
[31] R. A. Malfliet and J. Tjon, Nucl. Phys. **A127**, 161 (1969).
[32] T. W. Donnelly, Prog. Part. Nucl. Phys. **13**, 183 (1985).
[33] S. Boffi, C. Giusti, and F. D. Pacati, Phys. Rep. **226**, 1 (1993).
[34] M. L. Goldberger and K. M. Watson, *Collision Theory* (Wiley, New York, 1964).
[35] A. La Piana and W. Leidemann, Nucl. Phys. **A677**, 423 (2000).
[36] V. D. Efros, Yad. Fiz. **56, N7**, 22 (1993) [Phys. At. Nucl. **56**, 869 (1993)].
[37] V. D. Efros, Yad. Fiz. **62**, 1975 (1999) [Phys. At. Nucl. **62**, 1833 (1999)].
[38] M. A. Marchisio, N. Barnea, W. Leidemann, and G. Orlandini, Few-Body Syst. **33**, 259 (2003).
[39] V. D. Efros, W. Leidemann, and G. Orlandini, Few-Body Syst. **26**, 251 (1999).
[40] V. D. Efros, W. Leidemann, and G. Orlandini, Phys. Lett. **B408**, 1 (1997).
[41] B. A. Fomin and V. D. Efros, Yad. Fiz. **34**, 587 (1981) [Sov. J. Nucl. Phys. **34**, 327 (1981)].
[42] V. D. Efros, W. Leidemann, and G. Orlandini, Phys. Rev. C **58**, 582 (1998).
[43] R. Schiavilla, V. R. Pandharipande, and R. B. Wiringa, Nucl. Phys. **A449**, 219 (1986).
[44] R. B. Wiringa, Phys. Rev. C **43**, 1585 (1991).
[45] A. Arriaga, V. R. Pandharipande, and R. B. Wiringa, Phys. Rev. C **52**, 2362 (1995).
[46] R. Schiavilla, Phys. Rev. Lett. **65**, 835 (1990).
[47] J. Laget, Nucl. Phys. **A497**, 391c (1989).
[48] J. Golak, R. Skibinski, H. Witala, W. Glöckle, A. Nogga, and H. Kamada, Phys. Rep. **415**, 89 (2005).
[49] J. Golak, H. Kamada, H. Witala, W. Glöckle, and S. Ishikawa, Phys. Rev. C **51**, 1638 (1995) and private communication.